Published in final edited form as:
Am J Physiol Heart Circ Physiol. 2007 August ; 293(2): H909–H918.

Decreased age-related cardiac dysfunction, myocardial nitrative stress, inflammatory gene expression, and apoptosis in mice lacking fatty acid amide hydrolase

Sándor Bátkai[1,*], **Mohanraj Rajesh**[1,*], **Partha Mukhopadhyay**[1,*], **György Haskó**[2], **Lucas Liaudet**[3], **Benjamin F. Cravatt**[4], **Anna Csiszár**[5], **Zoltan Ungvári**[5], and **Pál Pacher**[1]

[1]*Sections on Oxidative Stress Tissue Injury, Laboratory of Physiological Studies, National Institute on Alcohol Abuse and Alcoholism, National Institutes of Health, Bethesda, Maryland* [2]*Department of Surgery, University of Medicine and Dentistry, New Jersey-New Jersey Medical School, Newark, New Jersey* [3]*Department of Intensive Care Medicine, University Hospital, Lausanne, Switzerland* [4]*The Skaggs Institute for Chemical Biology and Department of Cell Biology, The Scripps Research Institute, La Jolla, California* [5]*Department of Physiology, New York Medical College, Valhalla, New York*

Abstract

Recent studies have uncovered important cross talk between inflammation, generation of reactive oxygen and nitrogen species, and lipid metabolism in the pathogenesis of cardiovascular aging. Inhibition of the endocannabinoid anandamide metabolizing enzyme, the fatty acid amide hydrolase (FAAH), is emerging as a promising novel approach for the treatment of various inflammatory disorders. In this study, we have investigated the age-associated decline of cardiac function and changes in inflammatory gene expression, nitrative stress, and apoptosis in FAAH knockout ($FAAH^{-/-}$) mice and their wild-type ($FAAH^{+/+}$) littermates. Additionally, we have explored the effects of anandamide on TNF-α-induced ICAM-1 and VCAM-1 expression and monocyte-endothelial adhesion in human coronary artery endothelial cells (HCAECs). There was no difference in the cardiac function (measured by the pressure-volume conductance catheter system) between 2- to 3-mo-old (young) $FAAH^{-/-}$ and $FAAH^{+/+}$ mice. In contrast, the aging-associated decline in cardiac function and increased myocardial gene expression of TNF-α, gp91phox, matrix metalloproteinase (MMP)-2, MMP-9, caspase-3 and caspase-9, myocardial inducible nitric oxide synthase protein expression, nitrotyrosine formation, poly (ADP-ribose)polymerase cleavage and caspase-3/9 activity, observed in 28- to 31-mo-old (aging) $FAAH^{+/+}$ mice, were largely attenuated in knockouts. There was no difference in the myocardial cannabinoid CB_1 and CB_2 receptor gene expression between young and aging $FAAH^{-/-}$ and $FAAH^{+/+}$ mice. Anandamide dose dependently attenuated the TNF-α-induced ICAM-1 and VCAM-1 expression, NF-κB activation in HCAECs, and the adhesion of monocytes to HCAECs in a CB_1-and CB_2-dependent manner. These findings suggest that pharmacological inhibition of FAAH may represent a novel protective strategy against chronic inflammation, oxidative/nitrative stress, and apoptosis associated with cardiovascular aging and atherosclerosis.

Keywords

cardiac function; anandamide; pressure-volume relationship; endocannabinoids

Address for reprint requests and other correspondence: P. Pacher, Section on Oxidative Stress and Tissue Injury, Laboratory of Physiologic Studies, National Institutes of Health/NIAAA, 5625 Fishers Ln., MSC-9413, Bethesda, MD 20892-9413 (e-mail: pacher@mail.nih.gov).
*S. Bátkai, M. Rajesh, and P. Mukhopadhyay contributed equally to this study.

Modulation of the endocannabinoid system is emerging as a novel approach for the therapy of various inflammatory, metabolic, cardiovascular, gastrointestinal, liver, and neurodegenerative disorders (reviewed in Refs. 32,35,47). The natural ligands [endocannabinoids: arachidonoyl ethanolamide or anandamide (AEA) and 2-arachidonoylglycerol (2-AG)], similarly to their synthetic analogs, exert various anti-inflammatory and other effects mediated through the activation of two known cannabinoid (CB) receptors: the CB_1 receptor, which is highly expressed in the brain (40) but is also present in peripheral tissues including vascular tissues (25,34), heart (5,49), and liver (3,22,45,65), and the CB_2 receptor, previously thought to be expressed primarily in immune and hematopoietic cells (reviewed in Ref. 47). However, more recent studies have also identified CB_2 receptors in brain (67), myocardium (43), cardiomyoblasts (43,58), and endothelial cells of various origins (6,26,42,71; reviewed in Refs. 32,35,47).

Recent studies have revealed important cross talk between inflammation, generation of reactive oxygen and nitrogen species, and lipid metabolism in the pathogenesis of cardiovascular aging and atherosclerosis (13–16,27,50). Fatty acid amide hydrolase (FAAH), the enzyme responsible for the degradation of anandamide and related fatty acid amides in vivo, has emerged as a promising target for modulating endocannabinoid signaling, with a therapeutic potential in anxiety, pain, and various inflammatory disorders (e.g., colitis, arthritis, neurodegenerative disorders, atherosclerosis, etc.; reviewed in Refs. 11,32,35,47). Excitingly, a recent study has demonstrated that analogs of the nonsteroidal anti-inflammatory drugs indomethacin and ibuprofen are inhibitors of FAAH, suggesting that the combined FAAH-cyclooxygenase inhibitors may have therapeutic potential in various inflammatory disorders (29).

In this study, we have characterized the age-dependent decline of cardiac function and associated changes in myocardial inflammatory gene expression, nitrative stress, and apoptosis in FAAH knockout ($FAAH^{-/-}$) mice and their wild-type ($FAAH^{+/+}$) littermates. We have also investigated the effects of anandamide on TNF-α-induced intercellular adhesion molecule-1 (ICAM-1) and vascular adhesion molecule-1 (VCAM-1) expression and monocyte-endothelial adhesion in human coronary artery endothelial cells (HCAECs). These results indicate that 28- to 31-mo-old aging mice lacking FAAH have less myocardial oxidative/nitrative stress, inflammation, and apoptosis and better preservation of the cardiac function compared with their wild-type littermates. Furthermore, anandamide attenuates TNF-α-induced ICAM-1 and VCAM-1 expression, NF-κB activation in HCAECs, and the adhesion of monocytes to HCAECs in a CB_1- and CB_2-dependent manner.

MATERIALS AND METHODS

All protocols were approved by the National Institute on Alcohol Abuse and Alcoholism (NIAAA) Animal Care and Use Committee and were performed in accordance with the National Research Council's *Guide for the Care and Use of Laboratory Animals*.

Materials

1-(2,4-Dichlorophenyl)-5-(4-iodophenyl)-4-methyl-*N*-4-moepholinyl-1H-pyrazole-3-carboxamide (AM281), 6-iodo-2-methyl-1-[2-(4-morphoninyl)ethyl]-1H-indol-2-yl-(4-methoxyphenyl)methanone (AM630), and AEA were purchased from Tocris Bioscience (Ellisville, MO). Human recombinant TNF-α was obtained from R&D Systems. Unless otherwise specified, all other chemicals were purchased from Sigma (St. Louis, MO). Sources of antibodies are mentioned below, as appropriate.

Cell culture

HCAECs and growth medium were purchased from Cell Applications (San Diego, CA). HCAECs were used for the experiments between passages 3 and 7. The human monocytic cell line THP-1 was obtained from American Type Culture Collection and grown in RPMI 1640 medium supplemented with 2 mM L-glutamine, 10 mM HEPES, 10% FBS, 100 units/ml penicillin, and 100 μg/ml streptomycin, respectively. The cells were maintained at 37°C in a 5% CO_2 incubator as described previously (55).

Hemodynamic measurements

Young [2- to 3-mo-old male $FAAH^{-/-}$ (n = 20) and $FAAH^{+/+}$ (n = 21)] and aging [28- to 31-mo-old male $FAAH^{-/-}$ (n = 18) and $FAAH^{+/+}$ (n = 17)] mice weighing 22–36 g were used for the study. Left ventricular performance was analyzed in mice anesthetized with 2% isoflurane. The animals were placed on controlled heating pads, and core temperature measured via a rectal probe was maintained at 37°C. The trachea was cannulated, and the animals were artificially ventilated using a MiniVent respirator (Harvard Apparatus, Holliston, MA) at rates and tidal volumes adjusted to the body weights. A microtip pressure-volume catheter (SPR-839; Millar Instruments, Houston, TX) was inserted into the right carotid artery and advanced into the left ventricle as described previously (43,48,51). After stabilization for 20 min, the signals were continuously recorded at a sampling rate of 1,000 s^{-1} using an ARIA pressure-volume conductance system (Millar Instruments) coupled to a Powerlab/4SP analog-to-digital converter (AD Instruments, Mountain View, CA) and stored and displayed on a computer. All pressure-volume loop data were analyzed using a cardiac pressure-volume analysis program (PVAN3.5, Millar Instruments), and the heart rate, maximal left ventricular systolic pressure (LVSP), left ventricular end-diastolic pressure (LVEDP), maximal slope of systolic pressure increment (+dP/dt), diastolic decrement (−dP/dt), cardiac output, cardiac index, and stroke work were computed. The relaxation time constant (τ), an index of diastolic function, was also calculated by two different methods [Weiss method, regression of log (pressure) vs. time; Glantz method, regression of dP/dt vs. pressure]. All hemodynamic parameters were calculated and corrected according to in vitro and in vivo volume calibrations (43,48,49,51).

Real-time PCR analyses

Total RNA was isolated from tissue (heart) homogenate using Trizol LS reagents (Invitrogen, Carlsbad, CA) according to the manufacturer's instructions. The isolated RNA was treated with RNase-free DNase (Ambion, Austin, TX) to remove traces of genomic DNA contamination. Total RNA of 1 μg was reverse transcribed to cDNA using Super-Script II (Invitrogen). The target gene expression was quantified with iTaq SYBR Green mix (Bio-Rad, Hercules, CA), using the Bio-Rad Chromo 4/Opticon system. Each amplified sample in all wells was analyzed for homogeneity using melting curve analysis. Relative quantification was calculated using the comparative threshold cycle (C_T) method. Lower ΔC_T values and lower $\Delta\Delta C_T$ reflect a relatively higher amount of gene transcript. Statistical analyses were carried out for at least 6 –15 replicate experimental samples in each set.

The primers used were as follows: caspase-3, 5′-TGGACTGTGGCATTGAGACAG-3′ and 5′-CGACCCGTCCTTTGAATTTC-3′; caspase-9, 5′-GGATGCTGTGTCAAGTTTGCC-3′ and 5′-CTTTCGCAGAAACAGCATTGG-3′; gp91phox, 5′-GACCATTGCAAGTGAACACCC-3′ and 5′-AAATGAAGTGGACTCCACGCG-3′; matrix metalloproteinase-2 (MMP-2), 5′-CAAGGACCGGTTTATTTGGC-3′ and 5′-ATTCCCTGCGAAGAACACAGC-3′; MMP-9, 5′-TCTTCTGGCGTGTGAGTTTCC-3′ and 5′-CGGTTGAAGCAAAGAAGGAGC-3′; TNF-α, 5′-GCCTGTAGCCCACGTCGTA-3′ and 5′-GGTACAACCCATCGGCTGG-3′; CB_1 receptor, 5′-TCATGTGAAGGCACTGCGC-3′ and 5′-CAGCCACAAAAGCAGCAGG-3′; CB_2 receptor, 5′-

CCTTGCTTCGGTTTCCTTCTC-3′ and 5′-CACAAAGGTCTCCATGGTTGC-3′; and actin, 5′-TGCACCACCAACTGCTTAG-3′ and 5′-GGATGCAGGGATGATGTTC-3′.

Western immunoblot analyses

Protein was extracted from tissue homogenates using RIPA lysis buffer containing protease inhibitor cocktail set III (Calbiochem, EMD Biosciences, San Diego, CA) and phosphatase inhibitor cocktail set I (Calbiochem, EMD Biosciences). Protein was measured by the DC protein assay kit (Bio-Rad), and equal amounts (40 μg/lane) were fractionated on NuPAGE 4–12% Bis-Tris gel (Invitrogen) and transferred onto nitrocellulose membrane (Invitrogen) using a semidry transfer apparatus (Bio-Rad). The blocking was carried out for 2 h in 5% nonfat dry milk prepared in PBS. The primary antibodies were added according to the manufacturer's recommendation in 5% nonfat dry milk containing 0.1% Tween-20 for overnight at 4°C. After three washes in PBS containing 0.1% Tween-20, secondary horseradish peroxidase conjugate (Pierce Biotechnology, Rockford, IL) was added, followed by three washes with PBS containing 0.1% Tween-20. The blots were detected with Supersignal West Pico chemiluminescent substrate (Pierce Biotechnology) and developed using Kodak Biomax film (PerkinElmer, Wellesley, MA). Immunoblots were scanned with an Epson V750 Pro scanner, and quantification following background correction was carried out by ImageQuant5.1 software (Molecular Dynamics). All quantitative values were normalized to β-actin. Antibodies used were anti-actin mAb (Chemicon, Temecula, CA), anti-PARP (Cell Signaling), and anti-cleaved PARP and anti-inducible nitric oxide synthase (anti-iNOS) mAb (BD Biosciences).

Nitrotyrosine ELISA

Nitrotyrosine was quantified with an HBT Nitrotyrosine ELISA kit according to the manufacturer's instructions (Cell Sciences). Samples and standards were incubated in microtiter wells coated with antibodies recognizing nitrotyrosine. During this incubation, nitrotyrosine was captured by the solid bound antibody. Unbound material present in the sample was removed by washing. Biotinylated second antibody (tracer) to nitrotyrosine was added to the wells. Excess tracer was removed by washing. Streptavidin-peroxidase conjugate was applied to the wells; this conjugate reacts specifically with the biotinylated tracer antibody bound onto the detected nitrotyrosine. Excess streptavidin-peroxidase conjugate was removed by washing, and a substrate, tetramethylbenzidine (TMB), was added to the wells. Color developed proportionally to the amount of nitro-tyrosine present in the sample. The enzyme reaction was stopped by the addition of citric acid, and absorbance at 450 nm was measured with a spectrophotometer. A standard curve was obtained by plotting the absorbance vs. the corresponding concentrations of the nitrotyrosine standards. The nitrotyrosine concentration of samples with unknown concentrations, which were run concurrently with the standards, was determined from the standard curve.

Caspase-3/7 activity from myocardial tissue was determined as previously described (13,43).

Cell surface ICAM-1 and VCAM-1 expression assay

Cell surface expression of ICAM-1 and VCAM-1 was measured using in situ ELISA as has been described (55). In brief, HCAECs were grown in 96-well plates coated with 0.2% gelatin. After treatments, cells were washed with PBS three times and fixed in 4% formaldehyde in PBS (pH 7.4) for 30 min at 4°C. After being washed, the cells were blocked with PBS containing 1% bovine serum albumin and 0.1 M glycine for 2 h at 4°C. The fixed monolayer was incubated with either ICAM-1 or VCAM-1 monoclonal antibodies (R&D systems) at 1:1,000 dilutions for 1 h at 37°C. Next, the cells were incubated with peroxidase-conjugated anti-mouse secondary antibody (1:5,000; Pierce, IL) for 1 h at 37°C. After being washed, cells were incubated with 100 μl of developing substrate solution (3,3′,5,5′-tetramethylbenzidine)

for 10 min, and the reaction was terminated with 2 N H_2SO_4. Finally, the absorbance was measured at 450 nm using an ELISA reader (Molecular Devices). Each treatment was performed in duplicate, and the experiments were repeated three times.

Monocyte adhesion assay

Determination of monocyte adhesion to the endothelial cells was conducted using human THP-1 cells as previously described (55). In brief, HCAECs were grown to confluence in 24-well plates and treated with agonists/antagonists plus or minus TNF-α (see legend to Fig. 6 for description). THP-1 cells were labeled with 1.5 μM calcein-AM (Molecular Probes, Invitrogen) for 1 h at 37°C in RPMI 1640 containing 1% FBS. The cells were then washed two times with RPMI 1640 containing 1% FBS to remove the excess stain. Subsequently, the cells were re-suspended in HCAEC basal medium containing 2% FBS. HCAECs were washed twice with HCAEC basal medium and covered with 400 μl of HCAEC basal medium. Then, 10^5/100 μl labeled THP-1 cells were added to HCAECs and incubated for 1 h at 37°C in a 5% CO_2 incubator. After incubation, the medium containing monocytes was aspirated, and the monolayer was gently washed with PBS three times to remove the unbound monocytes. The adherent monocytes were documented using an Olympus IX 81 fluorescent microscope with ×10 objective. Three fields were documented per experimental condition. Individual treatments were performed in duplicate, and the set of experiments was repeated three times. The number of adherent THP-1 cells was counted using National Institutes of Health (NIH) Image J software, and the values were expressed as cells adhered per field.

NF-κB activation

NF-κB activation by TNF-α was determined by immunofluorescence assays by evaluating the nuclear translocation of p-65 (NF-κB). In brief, cells were grown in 0.2% gelatin-coated chamber slides (Labtek, Nalge Nunc). After treatments, cells were fixed in 4% paraformaldehyde for 30 min, followed by washing with PBS. Then they were permeabilized with 0.2% Triton X-100 (in PBS) for 20 min. Subsequently, cells were incubated with mouse anti-human NF-κB (p-65) (1:1,000 dilution, BD Biosciences) for 1 h at room temperature (RT). They were then probed with rabbit anti-mouse-FITC conjugate (1:1,000 dilution, Pierce Biotechnology) for 1 h at RT.

Statistical analyses

Strain- and time-dependent variables were analyzed by two-way ANOVA. Adjusted Student's *t*-test was used after ANOVA for pairwise comparisons, using GraphPad Prism (San Diego, CA). Significance was assumed if $P < 0.05$.

RESULTS

Cardiac function

Cardiac function was not significantly different in anesthetized young $FAAH^{-/-}$ and $FAAH^{+/+}$ mice, consistent with our previous report (Ref. 49; Fig. 1). Aging $FAAH^{+/+}$ mice had decreased indexes of systolic contractile function (LVSP, +dP/d*t*, cardiac output, cardiac index, and stroke work). In contrast, LVEDP and τ values were increased in aging $FAAH^{+/+}$ animals, and −dP/d*t* was decreased, indicating diastolic dysfunction (Fig. 1). The aging-associated systolic and diastolic dysfunction was less pronounced in aging $FAAH^{-/-}$ mice compared with $FAAH^{+/+}$ littermates (Fig. 1).

Cannabinoid CB_1 and CB_2 receptor gene expression was not different in the myocardial samples from young and aging $FAAH^{-/-}$ or $FAAH^{+/+}$ mice (Fig. 2, *A* and *B*). TNF-α and gp91phox (Fig. 2, *C* and *D*), MMP-2 and -9 (Fig. 3, *C* and *D*), and caspase-3 and -9 (Fig. 4,

C and *D*) gene expressions were markedly increased in myocardia of aging $FAAH^{+/+}$ mice but only moderately so in aging $FAAH^{-/-}$ mice (compared with corresponding young controls and with each other).

Myocardial iNOS protein expression (Fig. 3*A*), nitrotyrosine formation (Fig. 3*B*), cleaved PARP (Fig. 4*A*), and caspase-3/7 activity (Fig. 4*B*) were increased in myocardia of aging $FAAH^{+/+}$ mice but only moderately so in aging $FAAH^{-/-}$ mice (compared with corresponding young controls and with each other).

AEA mitigates TNF-α-induced ICAM-1 and VCAM-1 expression

TNF-α (50 ng/ml) treatment of HCAECs for 6 h led to marked upregulation of ICAM-1 (Fig. 5, *A* and *B*) and VCAM-1 (Fig. 5, *C* and *D*) expression. AEA pretreatment (0 –20 μM) dose dependently reduced ICAM-1 (Fig. 5*A*) and VCAM-1 (Fig. 5*C*) expressions. These effects were attenuated by AM281 and AM630 (CB_1 and CB_2 receptor antagonists), respectively (Fig. 5, *B* and *D*).

AEA mitigates TNF-α-induced monocyte adhesion to HCAECs

As shown in Fig. 6, TNF-α (50 ng/ml) treatment of HCAECs for 6 h led to a dramatic increase in monocyte adhesion when compared with controls. Pretreatment of cells with AEA (15 μM; starting from 1 h before and continuously present during the TNF-α exposure) inhibited TNF-α-induced monocyte adhesion to endothelial cells. This effect was attenuated by both AM281 and AM630 (Fig. 6).

AEA mitigates TNF-α-induced NF-κB activation in HCAECs

As depicted in Fig. 7, TNF-α induced marked activation of NF-κB in endothelial cells, mitigated by pretreatment with AEA, an effect that could be attenuated by CB_1 and CB_2 antagonists.

DISCUSSION

We demonstrate that mice lacking FAAH are more resistant to the age-associated decline in cardiac function compared with their wild-type littermates. Furthermore, the aging-associated increased myocardial gene expression of TNF-α, gp91phox, MMP-2, MMP-9, and caspase-3 and -9, myocardial iNOS protein expression, nitrotyrosine formation, PARP cleavage, and caspase-3/9 activity are also decreased in FAAH knockouts. We also show that anandamide dose dependently attenuates the TNF-α-induced ICAM-1 and VCAM-1 expression, NF-κB activation in HCAECs, and the adhesion of monocytes to HCAECs in a CB_1- and CB_2-dependent manner.

The existence of an anandamide-hydrolyzing enzyme was proposed by several groups (18, 21,28,66) shortly after the discovery of anandamide in 1992 (19). Consequently, the enzyme was purified and cloned (9,12), and FAAH knockout mice were developed (8). These mice have increased endogenous concentrations of anandamide and related fatty acid amides in the brain, liver, heart, and numerous other organs (8,41,49). $FAAH^{-/-}$ mice are characterized by increased CB_1-dependent hypoalgesia and hypersensitivity to the cannabinoid-like behavioral responses to exogenous anandamide (8), which can also be achieved by potent FAAH inhibitors (31). Importantly, neither pharmacological inhibition nor genetic deletion of the enzyme affects CB_1-regulated functions such as core body temperature and locomotion (8,31), suggesting that FAAH may represent an appealing therapeutic target for treating pain and related neurological disorders as well as anxiety, without the abuse potential of directly acting CB_1 agonists (reviewed in Refs. 10,20,47). Therefore, it is not surprising that there is considerable interest

in the development of novel potent FAAH inhibitors for various inflammatory disorders and other therapeutic indications (10,20,32,47).

$FAAH^{-/-}$ mice are protected against 2,4-dinitrobenzene sulfonic acid-induced colitis and develop a less severe inflammatory response and tissue injury (12a,37). This and recent studies with pharmacological inhibitors of cellular reuptake of anandamide (17) strongly suggest that upregulation of anandamide levels as an endogenous mechanism may be a feasible pharmacological strategy to limit inflammatory organ injury (reviewed in Refs. 20,32,47). There is also emerging evidence from in vitro studies suggesting that anandamide may inhibit NF-κB-dependent pivotal inflammatory pathways (induced by various inflammatory stimuli such as endotoxin and TNF-α) through cannabinoid receptor-dependent and -independent mechanisms (44,56). Consistent with these reports, we demonstrate for the first time that anandamide dose dependently attenuates TNF-α-induced adhesion molecule ICAM-1 and VCAM-1 expression, NF-κB activation in HCAECs, and the adhesion of monocytes to HCAECs in a CB_1- and CB_2-dependent manner.

Proinflammatory cytokines such as TNF-α play an important role in the cardiovascular aging process and mediate, at least in part, their proatherogenic effects by eliciting NF-κB activation in endothelial cells (13,27). The activation of this pathway leads to induction of adhesion molecules and chemokines, e.g., VCAM and ICAM-1 (69), which promote monocyte adhesiveness to the endothelium, and the release of a variety of factors that facilitate smooth muscle migration and proliferation to synthesize and deposit the extracellular matrix (27). There is considerable evidence suggesting that disruption of the cytokine-induced NF-κB signaling pathway confers a significant vasculoprotective effect by attenuating vascular inflammation (36,61), which delays or prevents atherogenesis in animal models (7,30,64) of disease. Disruption of this pathway with various cannabinoids may also exert significant protective effects by attenuating the endothelial cell activation, adhesion and activation of neutrophils and other inflammatory cells to the endothelium, and consequent inflammatory damage (4,36,55,56,62). These beneficial effects of cannabinoids could be therapeutically exploited in numerous cardiovascular disorders associated with increased inflammatory response, such as atherosclerosis, myocardial infarction, cardiac transplantation, and cardiovascular aging, to mention a few (reviewed in Refs. 32,33,46,47).

Numerous recent studies underscore the importance of the complex interplay between generation of reactive oxygen and nitrogen species, lipid metabolism, and inflammation in cardiovascular dysfunction associated with aging (reviewed in Refs. 14,50). TNF-α-induced superoxide generation might also favor increased expression of iNOS through the activation of NF-κB, which increases the generation of nitric oxide (NO). Superoxide anion reacts with NO to form the potent cytotoxin peroxynitrite, which attacks various biomolecules in the myocardium, vascular endothelium, and vascular smooth muscle, leading to cardiovascular dysfunction via multiple mechanisms including nitration of contractile proteins, impairment of mitochondrial function, activation of MMPs, and the nuclear enzyme poly(ADP-ribose) polymerase (to mention a few), eventually leading to cell death by apoptosis or necrosis and ultimately organ dysfunction (reviewed in Refs. 50,53,57). Consistent with previous mouse and rat studies, we show aging-associated decline of myocardial function (both systolic and diastolic) in aging $FAAH^{+/+}$ mice and increased gene expression of TNF-α, gp91phox, MMP-2, MMP-9, and caspase-3 and -9, myocardial iNOS protein expression, nitro-tyrosine formation, PARP cleavage, and caspase-3/9 activity (markers of oxidative/nitrative stress, inflammation, and apoptosis; Refs. 1,15,52,54,70). Remarkably, all the above-mentioned aging-associated changes were attenuated in $FAAH^{-/-}$ mice. It is tempting to speculate that increased anandamide levels might contribute (at least in part) to the above-mentioned anti-inflammatory phenotype observed in $FAAH^{-/-}$ mice by suppressing inflammatory pathways and interrelated oxidative/nitrative stress. It is noteworthy that anandamide may exert both proapoptotic (in

stellate cells and hepatocytes; Refs. 59,60) and anti-apoptotic effects (against serum deprivation in N18TG2 murine neuroblastoma cells; Ref. 38), determined by FAAH activity; however, this is a very controversial issue requiring further clarification. The myocardial levels of oleoylethanolamide are also increased in $FAAH^{-/-}$ mice (49), which could also be responsible for various protective effects in the cardiovascular system via multiple mechanisms [e.g., activation of Ras-Raf-1-Mek-Erk signaling pathway (63) and peroxisome proliferator-activated receptor-α (23), and direct antioxidant effects (2)]. It is important to note, however, that in addition to enzymatic hydrolysis, endocannabinoids are also susceptible to oxidative metabolism by a number of fatty acid oxygenases [e.g., cyclooxygenase, lipooxygenase, cytochrome *P*450 (68); reviewed in Ref. 39], and some of these metabolites are potent cardiovascular modulators (24). The effects of pharmacological inhibition or genetic inactivation of FAAH may thus be confounded by the activation of such alternative pathways of anandamide metabolism, particularly in the cardiovascular system, a possibility that needs to be explored in future studies.

Collectively, these findings suggest that pharmacological inhibition of FAAH may be of significant benefit in protecting against chronic inflammatory processes associated with cardiovascular aging and atherosclerosis, regardless of whether its beneficial effects are mediated by increased anandamide or oleoylethanolamide levels (or possibly other yet-unidentified biological substances metabolized by FAAH).

Acknowledgements

We are indebted to Millar Instruments for excellent customer support.

GRANTS

This study was supported by the Intramural Research Program of NIH/NIAAA (P. Pacher) and American Heart Association Grant No. 0435140N (A. Csiszár).

References

1. Adler A, Messina E, Sherman B, Wang Z, Huang H, Linke A, Hintze TH. NAD(P)H oxidase-generated superoxide anion accounts for reduced control of myocardial O_2 consumption by NO in old Fischer 344 rats. Am J Physiol Heart Circ Physiol 2003;285:H1015–H1022. [PubMed: 12915388]
2. Ambrosini A, Zolese G, Ambrosi S, Ragni L, Tiano L, Littarru G, Bertoli E, Mantero F, Boscaro M, Balercia G. Oleoylethanolamide protects human sperm cells from oxidation stress: studies on cases of idiopathic infertility. Biol Reprod 2006;74:659–665. [PubMed: 16354794]
3. Batkai S, Jarai Z, Wagner JA, Goparaju SK, Varga K, Liu J, Wang L, Mirshahi F, Khanolkar AD, Makriyannis A, Urbaschek R, Garcia N Jr, Sanyal AJ, Kunos G. Endocannabinoids acting at vascular CB1 receptors mediate the vasodilated state in advanced liver cirrhosis. Nat Med 2001;7:827–832. [PubMed: 11433348]
4. Batkai S, Osei-Hyiaman D, Pan H, El-Assal O, Rajesh M, Mukhopadhyay P, Hong F, Harvey-White J, Jafri A, Hasko G, Huffman JW, Gao B, Kunos G, Pacher P. Cannabinoid-2 receptor mediates protection against hepatic ischemia/reperfusion injury. FASEB J 2007;21:1788–1800. [PubMed: 17327359]
5. Batkai S, Pacher P, Osei-Hyiaman D, Radaeva S, Liu J, Harvey-White J, Offertaler L, Mackie K, Rudd MA, Bukoski RD, Kunos G. Endocannabinoids acting at cannabinoid-1 receptors regulate cardiovascular function in hypertension. Circulation 2004;110:1996–2002. [PubMed: 15451779]
6. Blazquez C, Casanova ML, Planas A, Del Pulgar TG, Villanueva C, Fernandez-Acenero MJ, Aragones J, Huffman JW, Jorcano JL, Guzman M. Inhibition of tumor angiogenesis by cannabinoids. FASEB J 2003;17:529–531. [PubMed: 12514108]
7. Branen L, Hovgaard L, Nitulescu M, Bengtsson E, Nilsson J, Jovinge S. Inhibition of tumor necrosis factor-alpha reduces atherosclerosis in apolipoprotein E knockout mice. Arterioscler Thromb Vasc Biol 2004;24:2137–2142. [PubMed: 15345516]

8. Cravatt BF, Demarest K, Patricelli MP, Bracey MH, Giang DK, Martin BR, Lichtman AH. Supersensitivity to anandamide and enhanced endogenous cannabinoid signaling in mice lacking fatty acid amide hydrolase. Proc Natl Acad Sci USA 2001;98:9371–9376. [PubMed: 11470906]

9. Cravatt BF, Giang DK, Mayfield SP, Boger DL, Lerner RA, Gilula NB. Molecular characterization of an enzyme that degrades neuromodulatory fatty-acid amides. Nature 1996;384:83–87. [PubMed: 8900284]

10. Cravatt BF, Lichtman AH. The endogenous cannabinoid system and its role in nociceptive behavior. J Neurobiol 2004;61:149–160. [PubMed: 15362158]

11. Cravatt BF, Lichtman AH. Fatty acid amide hydrolase: an emerging therapeutic target in the endocannabinoid system. Curr Opin Chem Biol 2003;7:469–475. [PubMed: 12941421]

12. Cravatt BF, Prospero-Garcia O, Siuzdak G, Gilula NB, Henriksen SJ, Boger DL, Lerner RA. Chemical characterization of a family of brain lipids that induce sleep. Science 1995;268:1506–1509. [PubMed: 7770779]

12a. Cravatt BF, Saghatelian A, Hawkins EG, Clement AB, Bracey MH, Lichtman AH. Functional disassociation of the central and peripheral fatty acid amide signaling systems. Proc Natl Acad Sci USA 2004;101:10821–10826. [PubMed: 15247426]

13. Csiszar A, Labinskyy N, Smith K, Rivera A, Orosz Z, Ungvari Z. Vasculoprotective effects of anti-tumor necrosis factor-alpha treatment in aging. Am J Pathol 2007;170:388–398. [PubMed: 17200210]

14. Csiszar A, Pacher P, Kaley G, Ungvari Z. Role of oxidative and nitrosative stress, longevity genes and poly(ADP-ribose) polymerase in cardiovascular dysfunction associated with aging. Curr Vasc Pharmacol 2005;3:285–291. [PubMed: 16026324]

15. Csiszar A, Ungvari Z, Edwards JG, Kaminski P, Wolin MS, Koller A, Kaley G. Aging-induced phenotypic changes and oxidative stress impair coronary arteriolar function. Circ Res 2002;90:1159–1166. [PubMed: 12065318]

16. Csiszar A, Ungvari Z, Koller A, Edwards JG, Kaley G. Aging-induced proinflammatory shift in cytokine expression profile in coronary arteries. FASEB J 2003;17:1183–1185. [PubMed: 12709402]

17. D'Argenio G, Valenti M, Scaglione G, Cosenza V, Sorrentini I, Di Marzo V. Up-regulation of anandamide levels as an endogenous mechanism and a pharmacological strategy to limit colon inflammation. FASEB J 2006;20:568–570. [PubMed: 16403786]

18. Deutsch DG, Chin SA. Enzymatic synthesis and degradation of anandamide, a cannabinoid receptor agonist. Biochem Pharmacol 1993;46:791–796. [PubMed: 8373432]

19. Devane WA, Hanus L, Breuer A, Pertwee RG, Stevenson LA, Griffin G, Gibson D, Mandelbaum A, Etinger A, Mechoulam R. Isolation and structure of a brain constituent that binds to the cannabinoid receptor. Science 1992;258:1946–1949. [PubMed: 1470919]

20. Di Marzo V, Bifulco M, De Petrocellis L. The endocannabinoid system and its therapeutic exploitation. Nat Rev Drug Discov 2004;3:771–784. [PubMed: 15340387]

21. Di Marzo V, Fontana A, Cadas H, Schinelli S, Cimino G, Schwartz JC, Piomelli D. Formation and inactivation of endogenous cannabinoid anandamide in central neurons. Nature 1994;372:686–691. [PubMed: 7990962]

22. Engeli S, Bohnke J, Feldpausch M, Gorzelniak K, Janke J, Batkai S, Pacher P, Harvey-White J, Luft FC, Sharma AM, Jordan J. Activation of the peripheral endocannabinoid system in human obesity. Diabetes 2005;54:2838–2843. [PubMed: 16186383]

23. Fu J, Oveisi F, Gaetani S, Lin E, Piomelli D. Oleoylethanolamide, an endogenous PPAR-alpha agonist, lowers body weight and hyperlipidemia in obese rats. Neuropharmacology 2005;48:1147–1153. [PubMed: 15910890]

24. Gauthier KM, Baewer DV, Hittner S, Hillard CJ, Nithipatikom K, Reddy DS, Falck JR, Campbell WB. Endothelium-derived 2-arachido-nylglycerol: an intermediate in vasodilatory eicosanoid release in bovine coronary arteries. Am J Physiol Heart Circ Physiol 2005;288:H1344–H1351. [PubMed: 15528233]

25. Gebremedhin D, Lange AR, Campbell WB, Hillard CJ, Harder DR. Cannabinoid CB1 receptor of cat cerebral arterial muscle functions to inhibit L-type Ca^{2+} channel current. Am J Physiol Heart Circ Physiol 1999;276:H2085–H2093.

26. Golech SA, McCarron RM, Chen Y, Bembry J, Lenz F, Mechoulam R, Shohami E, Spatz M. Human brain endothelium: coexpression and function of vanilloid and endocannabinoid receptors. Brain Res Mol Brain Res 2004;132:87–92. [PubMed: 15548432]
27. Hansson GK, Libby P. The immune response in atherosclerosis: a double-edged sword. Nat Rev Immunol 2006;6:508–519. [PubMed: 16778830]
28. Hillard CJ, Wilkison DM, Edgemond WS, Campbell WB. Characterization of the kinetics and distribution of N-arachidonylethanolamine (anandamide) hydrolysis by rat brain. Biochim Biophys Acta 1995;1257:249–256. [PubMed: 7647100]
29. Holt S, Paylor B, Boldrup L, Alajakku K, Vandevoorde S, Sundstrom A, Cocco MT, Onnis V, Fowler CJ. Inhibition of fatty acid amide hydrolase, a key endocannabinoid metabolizing enzyme, by analogues of ibuprofen and indomethacin. Eur J Pharmacol 2007;565:26–36. [PubMed: 17397826]
30. Jawien J, Gajda M, Mateuszuk L, Olszanecki R, Jakubowski A, Szlachcic A, Korabiowska M, Korbut R. Inhibition of nuclear factor-kappaB attenuates artherosclerosis in apoE/LDLR-double knockout mice. J Physiol Pharmacol 2005;56:483–489. [PubMed: 16204769]
31. Kathuria S, Gaetani S, Fegley D, Valino F, Duranti A, Tontini A, Mor M, Tarzia G, La Rana G, Calignano A, Giustino A, Tattoli M, Palmery M, Cuomo V, Piomelli D. Modulation of anxiety through blockade of anandamide hydrolysis. Nat Med 2003;9:76–81. [PubMed: 12461523]
32. Klein TW. Cannabinoid-based drugs as anti-inflammatory therapeutics. Nat Rev Immunol 2005;5:400–411. [PubMed: 15864274]
33. Lamontagne D, Lepicier P, Lagneux C, Bouchard JF. The endogenous cardiac cannabinoid system: a new protective mechanism against myocardial ischemia. Arch Mal Coeur Vaiss 2006;99:242–246. [PubMed: 16618028]
34. Liu J, Gao B, Mirshahi F, Sanyal AJ, Khanolkar AD, Makriyannis A, Kunos G. Functional CB1 cannabinoid receptors in human vascular endothelial cells. Biochem J 2000;346:835–840. [PubMed: 10698714]
35. Mackie K. Cannabinoid receptors as therapeutic targets. Annu Rev Pharmacol Toxicol 2006;46:101–122. [PubMed: 16402900]
36. Marui N, Offermann MK, Swerlick R, Kunsch C, Rosen CA, Ahmad M, Alexander RW, Medford RM. Vascular cell adhesion molecule-1 (VCAM-1) gene transcription and expression are regulated through an antioxidant-sensitive mechanism in human vascular endothelial cells. J Clin Invest 1993;92:1866–1874. [PubMed: 7691889]
37. Massa F, Marsicano G, Hermann H, Cannich A, Monory K, Cravatt BF, Ferri GL, Sibaev A, Storr M, Lutz B. The endogenous cannabinoid system protects against colonic inflammation. J Clin Invest 2004;113:1202–1209. [PubMed: 15085199]
38. Matas D, Juknat A, Pietr M, Klin Y, Vogel Z. Anandamide protects from low serum-induced apoptosis via its degradation to ethanolamine. J Biol Chem 2007;282:7885–7892. [PubMed: 17227767]
39. Matias I, Chen J, De Petrocellis L, Bisogno T, Ligresti A, Fezza F, Krauss AH, Shi L, Protzman CE, Li C, Liang Y, Nieves AL, Kedzie KM, Burk RM, Di Marzo V, Woodward DF. Prostaglandin ethanolamides (prostamides): in vitro pharmacology and metabolism. J Pharmacol Exp Ther 2004;309:745–757. [PubMed: 14757851]
40. Matsuda LA, Lolait SJ, Brownstein MJ, Young AC, Bonner TI. Structure of a cannabinoid receptor and functional expression of the cloned cDNA. Nature 1990;346:561–564. [PubMed: 2165569]
41. McKinney MK, Cravatt BF. Structure and function of fatty acid amide hydrolase. Annu Rev Biochem 2005;74:411–432. [PubMed: 15952893]
42. Mestre L, Correa F, Docagne F, Clemente D, Guaza C. The synthetic cannabinoid WIN 55,212-2 increases COX-2 expression and PGE2 release in murine brain-derived endothelial cells following Theiler's virus infection. Biochem Pharmacol 2006;72:869–880. [PubMed: 16914119]
43. Mukhopadhyay P, Batkai S, Rajesh M, Czifra N, Harvey-White J, Hasko G, Zsengeller Z, Gerard NP, Liaudet L, Kunos G, Pacher P. Pharmacological inhibition of cannabinoid receptor-1 protects against doxorubicin-induced cardiotoxicity. JACC. In press
44. Nakajima Y, Furuichi Y, Biswas KK, Hashiguchi T, Kawahara K, Yamaji K, Uchimura T, Izumi Y, Maruyama I. Endocannabinoid, anandamide in gingival tissue regulates the periodontal inflammation through NF-kappaB pathway inhibition. FEBS Lett 2006;580:613–619. [PubMed: 16406050]

45. Osei-Hyiaman D, DePetrillo M, Pacher P, Liu J, Radaeva S, Batkai S, Harvey-White J, Mackie K, Offertaler L, Wang L, Kunos G. Endocannabinoid activation at hepatic CB1 receptors stimulates fatty acid synthesis and contributes to diet-induced obesity. J Clin Invest 2005;115:1298–1305. [PubMed: 15864349]
46. Pacher P, Batkai S, Kunos G. Cardiovascular pharmacology of cannabinoids. Handb Exp Pharmacol 2005;168:599–625. [PubMed: 16596789]
47. Pacher P, Batkai S, Kunos G. The endocannabinoid system as an emerging target of pharmacotherapy. Pharmacol Rev 2006;58:389–462. [PubMed: 16968947]
48. Pacher P, Batkai S, Kunos G. Haemodynamic profile and responsiveness to anandamide of TRPV1 receptor knock-out mice. J Physiol 2004;558:647–657. [PubMed: 15121805]
49. Pacher P, Batkai S, Osei-Hyiaman D, Offertaler L, Liu J, Harvey-White J, Brassai A, Jarai Z, Cravatt BF, Kunos G. Hemodynamic profile, responsiveness to anandamide, and baroreflex sensitivity of mice lacking fatty acid amide hydrolase. Am J Physiol Heart Circ Physiol 2005;289:H533–H541. [PubMed: 15821037]
50. Pacher P, Beckman JS, Liaudet L. Nitric oxide and peroxynitrite in health and disease. Physiol Rev 2007;87:315–424. [PubMed: 17237348]
51. Pacher P, Liaudet L, Bai P, Mabley JG, Kaminski PM, Virag L, Deb A, Szabo E, Ungvari Z, Wolin MS, Groves JT, Szabo C. Potent metalloporphyrin peroxynitrite decomposition catalyst protects against the development of doxorubicin-induced cardiac dysfunction. Circulation 2003;107:896–904. [PubMed: 12591762]
52. Pacher P, Mabley JG, Liaudet L, Evgenov OV, Marton A, Hasko G, Kollai M, Szabo C. Left ventricular pressure-volume relationship in a rat model of advanced aging-associated heart failure. Am J Physiol Heart Circ Physiol 2004;287:H2132–H2137. [PubMed: 15231502]
53. Pacher P, Schulz R, Liaudet L, Szabo C. Nitrosative stress and pharmacological modulation of heart failure. Trends Pharmacol Sci 2005;26:302–310. [PubMed: 15925705]
54. Pacher P, Vaslin A, Benko R, Mabley JG, Liaudet L, Hasko G, Marton A, Batkai S, Kollai M, Szabo C. A new, potent poly(ADP-ribose) polymerase inhibitor improves cardiac and vascular dysfunction associated with advanced aging. J Pharmacol Exp Ther 2004;311:485–491. [PubMed: 15213249]
55. Rajesh M, Mukhopadhyay P, Batkai S, Hasko G, Liaudet L, Drel VR, Obrosova I, Pacher P. Cannabidiol attenuates high glucose-induced endothelial cell inflammatory response and barrier disruption. Am J Physiol Heart Circ Physiol. 10.1152/ajpheart.00373.2007First published April 13, 2007
56. Sancho R, Calzado MA, Di Marzo V, Appendino G, Munoz E. Anandamide inhibits nuclear factor-kappaB activation through a cannabinoid receptor-independent pathway. Mol Pharmacol 2003;63:429–438. [PubMed: 12527815]
57. Schulz R. Intracellular targets of matrix metalloproteinase-2 in cardiac disease: rationale and therapeutic approaches. Annu Rev Pharmacol Toxicol 2007;47:211–242. [PubMed: 17129183]
58. Shmist YA, Goncharov I, Eichler M, Shneyvays V, Isaac A, Vogel Z, Shainberg A. Delta-9-tetrahydrocannabinol protects cardiac cells from hypoxia via CB2 receptor activation and nitric oxide production. Mol Cell Biochem 2006;283:75–83. [PubMed: 16444588]
59. Siegmund SV, Seki E, Osawa Y, Uchinami H, Cravatt BF, Schwabe RF. Fatty acid amide hydrolase determines anandamide-induced cell death in the liver. J Biol Chem 2006;281:10431–10438. [PubMed: 16418162]
60. Siegmund SV, Uchinami H, Osawa Y, Brenner DA, Schwabe RF. Anandamide induces necrosis in primary hepatic stellate cells. Hepatology 2005;41:1085–1095. [PubMed: 15841466]
61. Spiecker M, Darius H, Liao JK. A functional role of I kappa B-epsilon in endothelial cell activation. J Immunol 2000;164:3316–3322. [PubMed: 10706725]
62. Steffens S, Veillard NR, Arnaud C, Pelli G, Burger F, Staub C, Karsak M, Zimmer A, Frossard JL, Mach F. Low dose oral cannabinoid therapy reduces progression of atherosclerosis in mice. Nature 2005;434:782–786. [PubMed: 15815632]
63. Su HF, Samsamshariat A, Fu J, Shan YX, Chen YH, Piomelli D, Wang PH. Oleylethanolamide activates Ras-Erk pathway and improves myocardial function in doxorubicin-induced heart failure. Endocrinology 2006;147:827–834. [PubMed: 16269455]

64. Takeda R, Suzuki E, Satonaka H, Oba S, Nishimatsu H, Omata M, Fujita T, Nagai R, Hirata Y. Blockade of endogenous cytokines mitigates neointimal formation in obese Zucker rats. Circulation 2005;111:1398–1406. [PubMed: 15781751]

65. Teixeira-Clerc F, Julien B, Grenard P, Tran Van Nhieu J, Deveaux V, Li L, Serriere-Lanneau V, Ledent C, Mallat A, Lotersztajn S. CB1 cannabinoid receptor antagonism: a new strategy for the treatment of liver fibrosis. Nat Med 2006;12:671–676. [PubMed: 16715087]

66. Ueda N, Kurahashi Y, Yamamoto S, Tokunaga T. Partial purification and characterization of the porcine brain enzyme hydrolyzing and synthesizing anandamide. J Biol Chem 1995;270:23823–23827. [PubMed: 7559559]

67. Van Sickle MD, Duncan M, Kingsley PJ, Mouihate A, Urbani P, Mackie K, Stella N, Makriyannis A, Piomelli D, Davison JS, Marnett LJ, Di Marzo V, Pittman QJ, Patel KD, Sharkey KA. Identification and functional characterization of brainstem cannabinoid CB2 receptors. Science 2005;310:329–332. [PubMed: 16224028]

68. Weber A, Ni J, Ling KH, Acheampong A, Tang-Liu DD, Burk R, Cravatt BF, Woodward D. Formation of prostamides from anandamide in FAAH knockout mice analyzed by HPLC with tandem mass spectrometry. J Lipid Res 2004;45:757–763. [PubMed: 14729864]

69. Wung BS, Ni CW, Wang DL. ICAM-1 induction by TNFalpha and IL-6 is mediated by distinct pathways via Rac in endothelial cells. J Biomed Sci 2005;12:91–101. [PubMed: 15864742]

70. Yang B, Larson DF, Watson RR. Modulation of iNOS activity in age-related cardiac dysfunction. Life Sci 2004;75:655–667. [PubMed: 15172175]

71. Zoratti C, Kipmen-Korgun D, Osibow K, Malli R, Graier WF. Anan-damide initiates Ca(2+) signaling via CB2 receptor linked to phospholipase C in calf pulmonary endothelial cells. Br J Pharmacol 2003;140:1351–1362. [PubMed: 14645143]

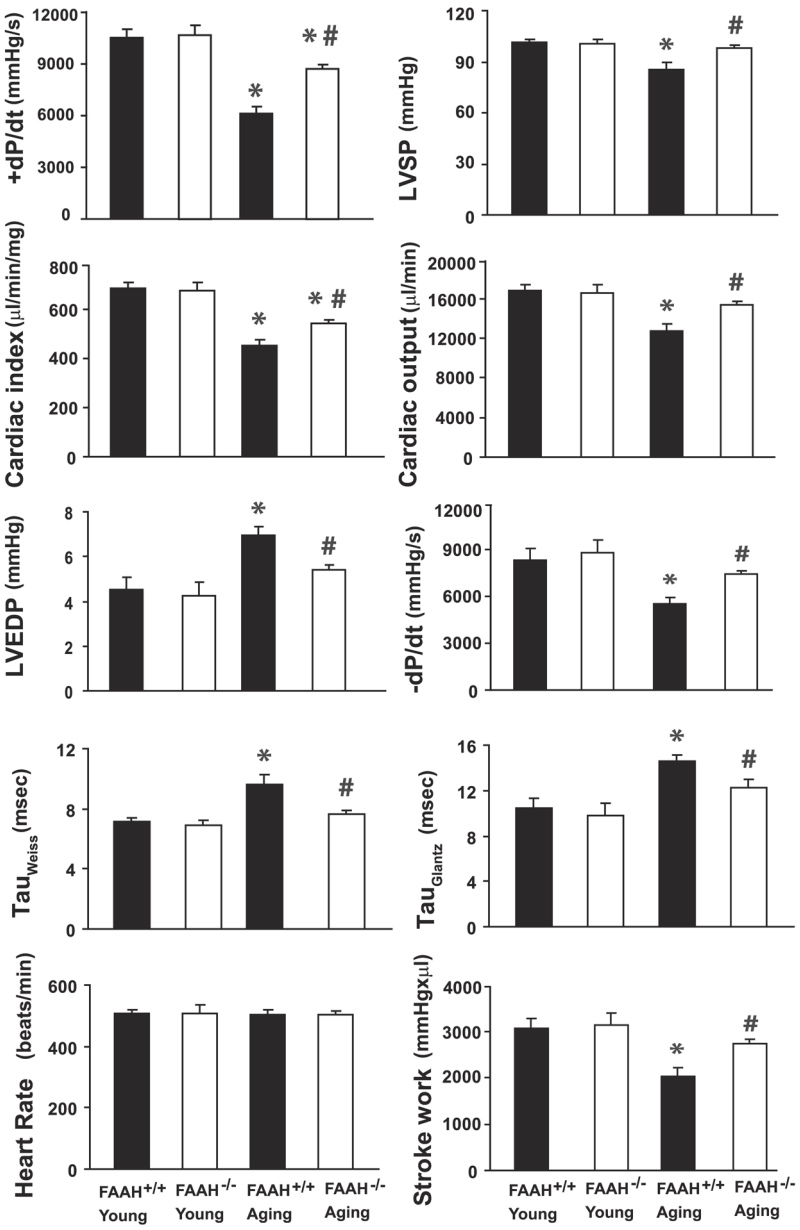

Fig. 1.

Hemodynamics in young (2- to 3-mo-old) and aging (28-to 31-mo-old) mice measured by the Millar pressure-volume conductance catheter system. Values are means ± SE of 7–11 experiments in each group. LVEDP, left ventricular end-diastolic pressure; LVSP, left ventricular systolic pressure; −dP/d*t*, diastolic decrement; tau (τ), relaxation time constant; FAAH, fatty acid amide hydrolase. **P* < 0.05 vs. young mice; #*P* < 0.05 vs. aging $FAAH^{+/+}$ mice.

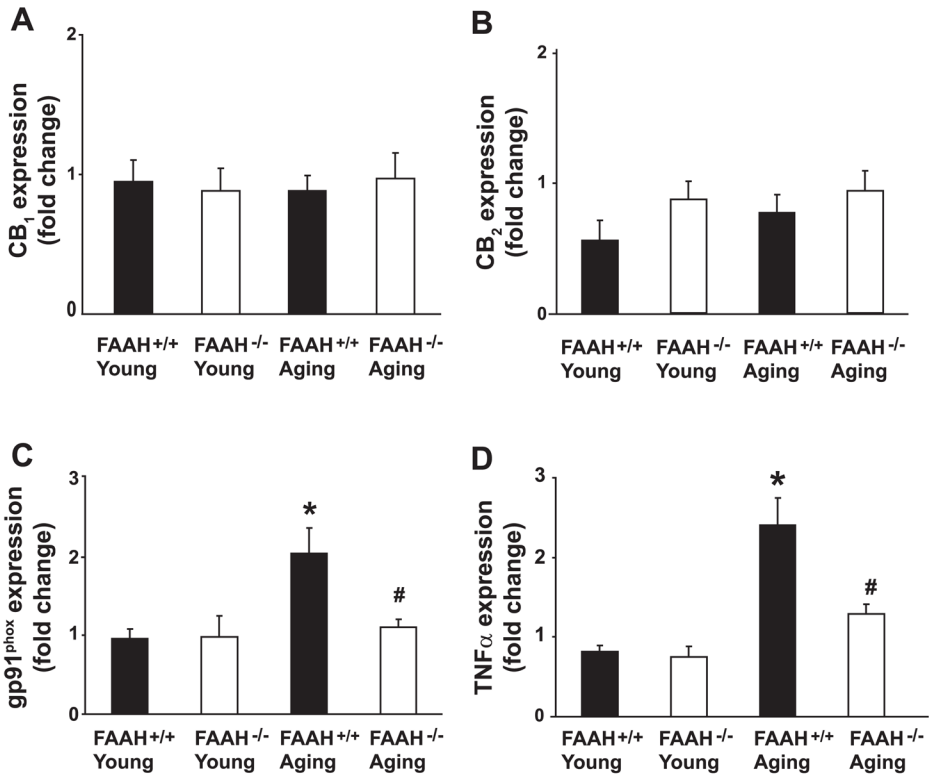

Fig. 2.

Myocardial cannabinoid CB_1 and CB_2 receptors, gp91phox, and TNF-α gene expression. Values are means ± SE of 6–15 experiments in each group. *$P < 0.05$ vs. young mice; #$P < 0.05$ vs. aging $FAAH^{+/+}$ mice.

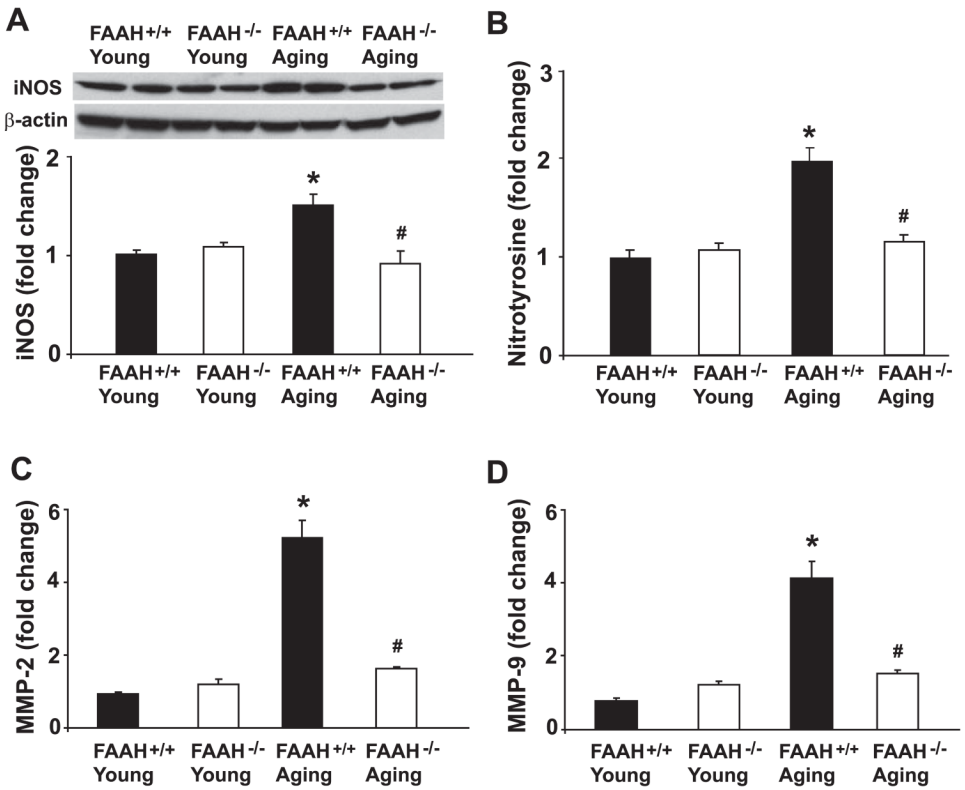

Fig. 3.

Myocardial inducible nitric oxide synthase (iNOS) protein expression, nitrotyrosine formation, and matrix metalloproteinase (MMP)-2 and -9 gene expression. Values are means ± SE of 5–15 experiments in each group. **P* < 0.05 vs. young mice; #*P* < 0.05 vs. aging FAAH$^{+/+}$ mice.

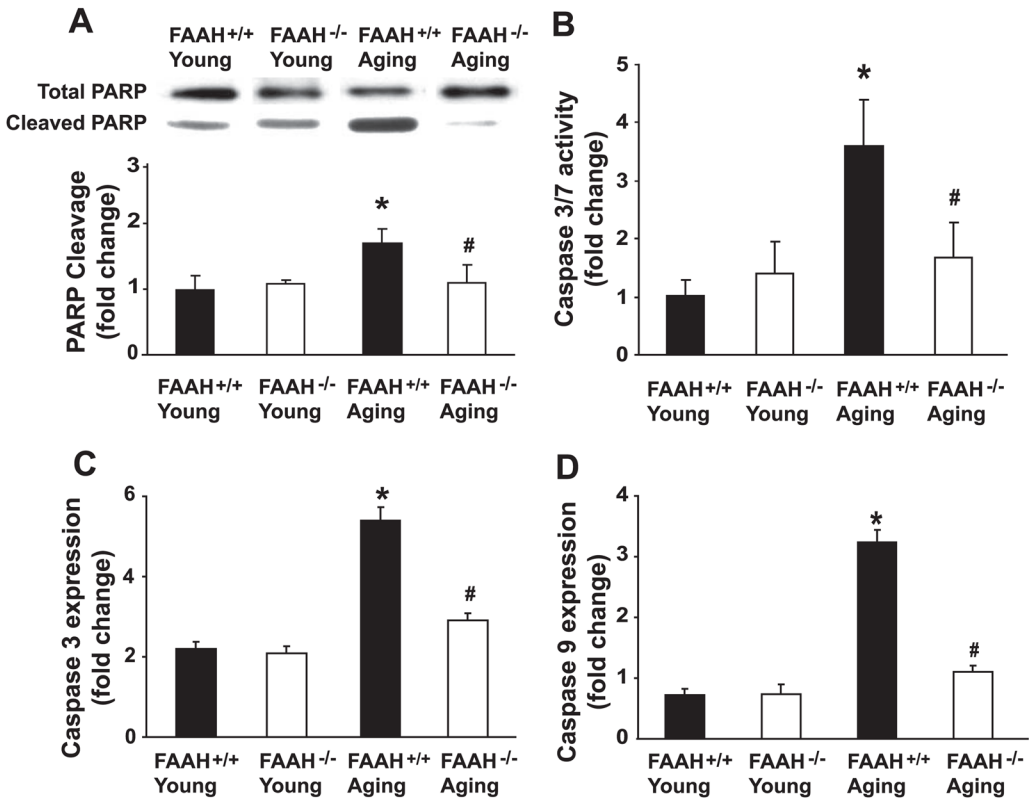

Fig. 4.

Myocardial markers of apoptosis (PARP cleavage, caspase-3/7 activity, and caspase-3 and -9 gene expression). Values are means ± SE of 5–15 experiments in each group. **P* < 0.05 vs. young mice; #*P* < 0.05 vs. aging $FAAH^{+/+}$ mice.

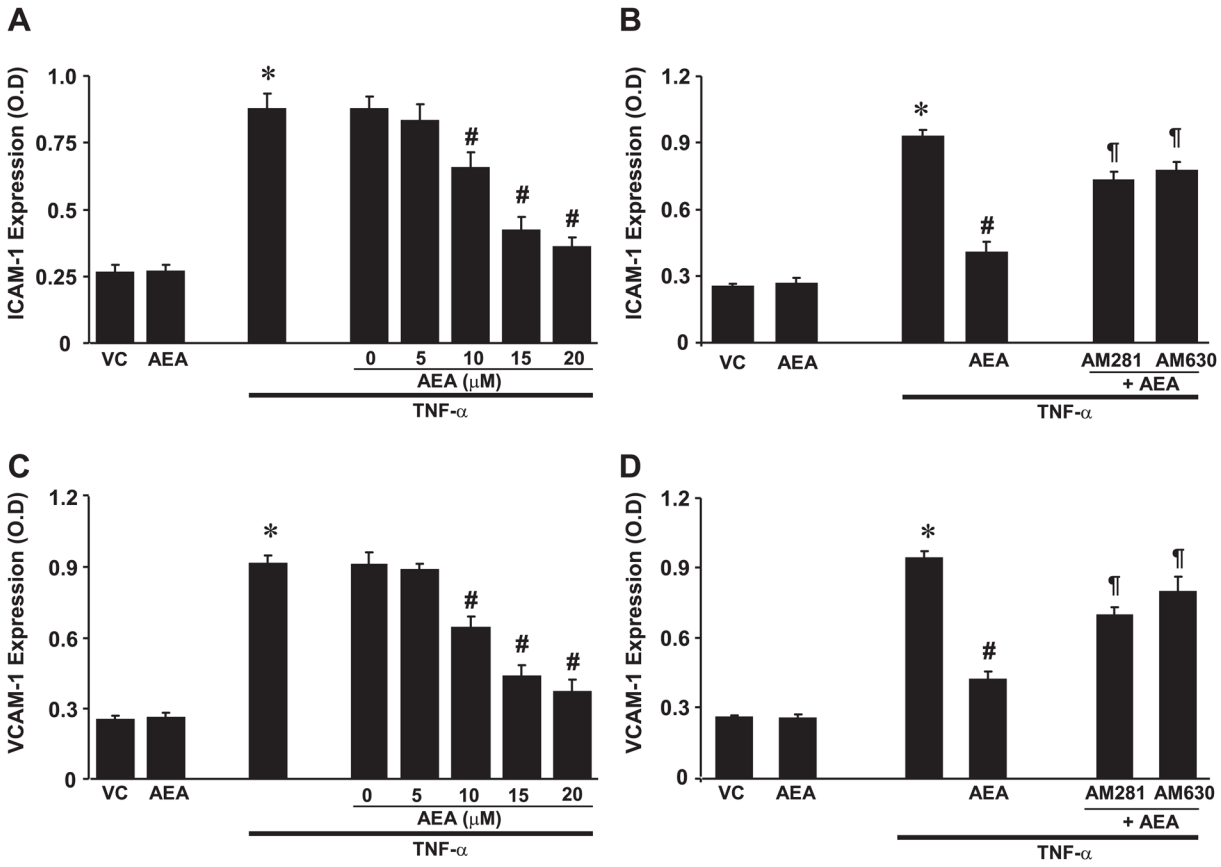

Fig. 5.

Effect of anandamide (AEA) on TNF-α-induced ICAM-1 and VCAM-1 expression in human coronary artery endothelial cells (HCAECs). Values are means ± SE; $n = 6$. Cells were treated with either TNF-α (50 ng/ml) or AEA (15 μM) for 6 h or pretreated with AEA with the indicated concentrations followed by treatment with TNF-α for 6 h, and then cell surface ELISA was performed as described in MATERIALS AND METHODS (*A* and *B*). VC, vehicle control. *A*: ICAM-1 expression. *$P < 0.05$ vs. controls; #$P < 0.05$ vs. TNF-α. *B*: VCAM-1 expression. *$P < 0.05$ vs. controls; #$P < 0.05$ vs. TNF-α. Cells were pretreated with CB_1/CB_2 antagonists (1 μM) from 1 h before and during the treatment with TNF-α ± AEA (15 μM) as indicated for 6 h, and cell surface ELISA was performed (*C* and *D*). *C*: ICAM-1 expression. *$P < 0.05$ vs. control; #$P < 0.05$ vs. TNF-α. Paragraph symbol: *P*g< 0.05 vs. AEA + TNF-α. *D*: VCAM-1 expression. *$P < 0.05$ vs. control; #$P < 0.05$ vs. TNF-α. Paragraph symbol: $P < 0.05$ vs. AEA + TNF-α.

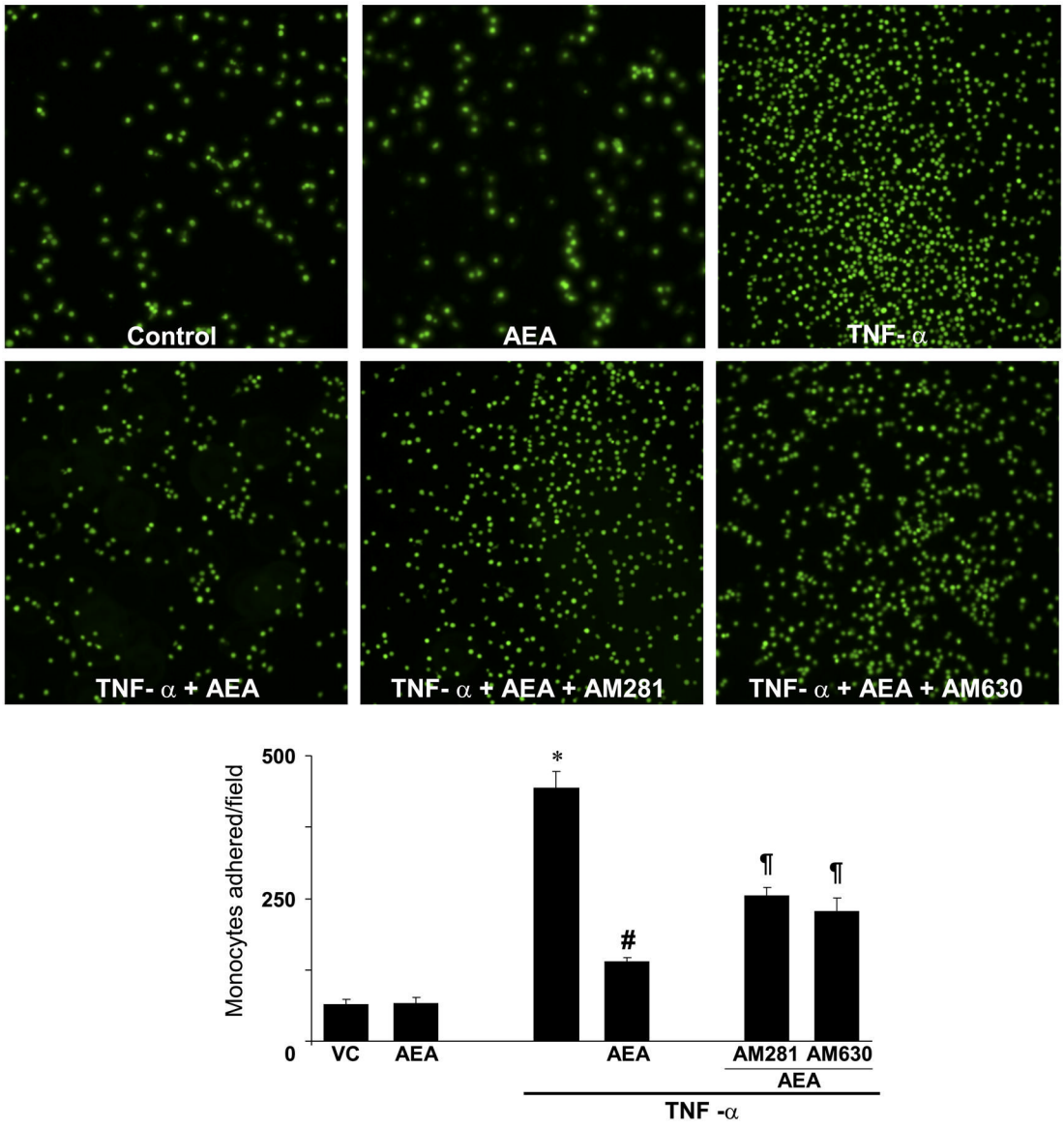

Fig. 6.

Effect of AEA on TNF-α-induced monocyte adhesion to HCAECs. HCAECs were treated as described in legend to Fig. 5. *Top*: representative images depicting monocytes adhered to the endothelial cells. *Bottom*: quantification of monocyte adhesion to endothelial cells. Values are means ± SE; $n = 6$. *$P < 0.05$ vs. control; #$P < 0.05$ vs. TNF-α. Paragraph symbol: $P < 0.05$ vs. AEA + TNF-α.

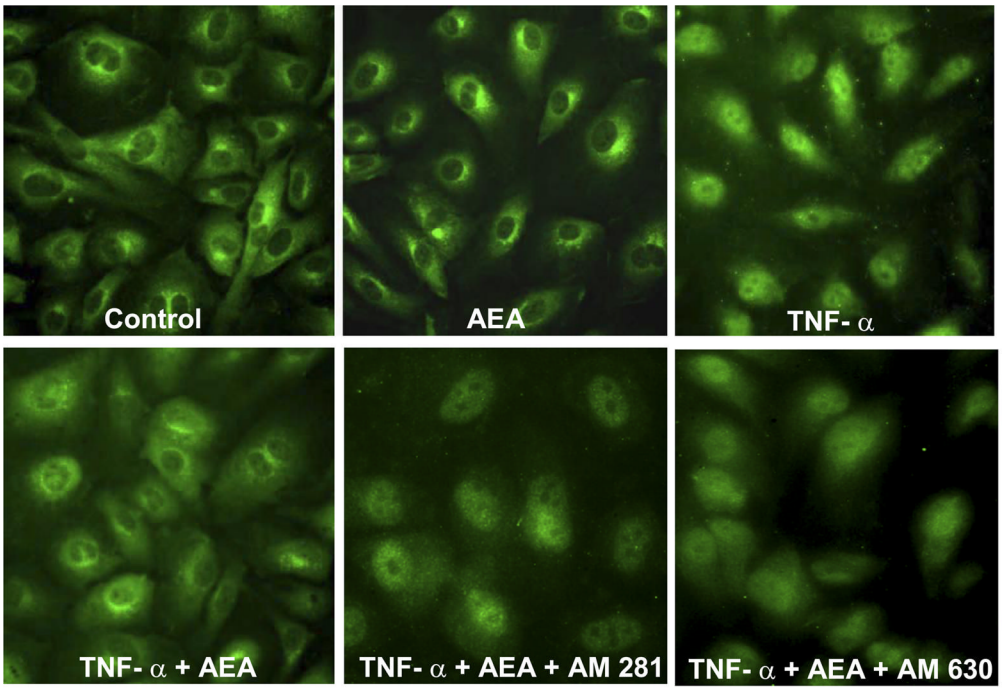

Fig. 7.

Effect of AEA on TNF-α-induced NF-κB activation in HCAECs. Representative immunofluorescence images of NF-κB activation in endothelial cells. TNF-α markedly activated NF-κB (note the intense nuclear staining). AEA significantly inhibits TNF-α-induced activation of NF-κB. Images shown are representative of 3 independent experiments yielding identical results.